Proc Indian Natn Sci Acad **72** No.2 pp. 97-111 (2006)

Review Article

Bulk Nanoceramic Composites for Structural Applications: A Review

AMARTYA MUKHOPADHYAY and BIKRAMJIT BASU*
Laboratory for Advanced Ceramics, Department of Materials and Metallurgical Engineering, Indian Institute of Technology, Kanpur-208016

(Received on 9 January 2006; Accepted on 31 May 2006)

With the recognition that the nanocrystalline ceramics, having grain sizes typically smaller than 100 nm, posses some appealing mechanical, physical, chemical and tribological properties, they have been the subject of considerable research activities in recent years. Considering the challenges involved in the processing of bulk ceramic nanomaterials, the research on nanostructured ceramics and composites was triggered with the advent of some advanced sintering techniques like, Field Assisted Sintering Techniques (FAST). This review paper presents an overview of the classification of ceramic nanocomposites, analyses some of the major challenges involved in the processing of these materials and in particular, discusses the use of FAST technique in processing nanoceramic materials. This contribution is also designed to highlight the improvement in mechanical properties, over conventional ceramics, and to provide a discussion on the processing-microstructures-mechanical properties of some selected oxide and non-oxide nanoceramic composites. Additionally, the limited literature reports covering the tribological properties of some of the nanocomposites is discussed. At the end, the unresolved issues concerned with the properties of nanoceramics and the scopes for future work have been touched upon.

Key Words: Nanomaterials, Nanoceramic composite, Spark plasma sintering, Mechanical properties, Superplasticity, Tribological properties

Introduction

Nanostructured materials are conventionally defined as materials exhibiting a characteristic length scale of the order of less than a hundred nanometers in any dimension. This length scale could refer to particle diameter, grain size, layer thickness or the width of a conducting line on an electronic chip. The fact that nanostructured materials show superior properties in comparison to conventional micronsized materials, as well as some unique properties, has triggered a significant research activity on the synthesis and characterization of the former. The extensive research efforts have led to some understanding of the behaviour of nanomaterials and hence rendering them suitable for several 'high-tech' applications.

Nanomaterials research was instigated by the possibility of utilizing the increased surface area to volume ratio in applications requiring surface chemical reactivity for uses such as catalysts [1] or pigments [2]. In addition to the betterment of chemical properties, it has been recognized that reduction of microstructural length scale to nanometer range could result in a modest improvement in the physical and mechanical properties of materials. The examples of such property improvement in selected ceramic systems are cited in subsequent sections.

It is well known that the structure of grain boundaries plays an important role in determining the mechanical and deformation behaviour of polycrystalline materials. At the microscopic level, ultra fine grain sizes and corresponding increase in the interface areas in nanostructured materials result in the presence of a significant fraction of atoms at the grain boundary environment and resultantly, the atomic arrangement at a grain boundary (GB) in a nanomaterial is different from that within a grain. It has been estimated that around 14-27% of all atoms reside in a region within 0.5-1 nm of a grain boundary for a grain size of 10 nm[3]. Generally the atoms at the grain boundaries occupy positions relaxed from their normal lattice sites and hence the properties of nanomaterial vary with the structure of the interfaces. As expected, the reduction of grain sizes leads to a substantial increase in strength. Apart from the advantages obtained due to superior strength, another unique property of materials with nanoscaled microstructure is that they can be superplastically deformed at high temperatures, by a mechanism primarily involving grain boundary sliding. This property can be particularly useful for shaping of otherwise brittle ceramics. Among ceramics, yttria stabilized tetragonal zirconia polycrystals (Y-TZP) have been shown to exhibit superplasticity at near nanocrystalline grain sizes [4,5,6]. Besides Y-TZP, the superplastic behavior has also been experimentally observed by Y-TZP-Al_2O_3 composites [7], Al_2O_3-ZrO_2 nanocomposites [8] and Si_3N_4-SiC nanocomposites [9] at temperatures of around 1400^0C.

* *Author for correspondence – E-mail: bikram@iitk.ac.in; Fax: 0091-512-2598591*

Apart from the mechanical properties, some physical properties, resulting from the reduced microstructural and macrostructural scale, can be exploited to processing benefits. For example, the refinement of microstructural length scale results in lowering of melting temperature [10]. Similarly, a reduction of powder particle sizes to nanometric dimensions result in considerable increase in surface area, aiding in faster mass transport during sintering (Herring's scaling law) [11].

The successful synthesis of these materials for the variety of applications requires the adoption of advanced processing techniques, which have been developed as a result of extensive research. The advanced sintering techniques, in particular using "Field Assisted Sintering Techniques" (FAST), rapid solidification, mechanical attrition, severe mechanical deformation, physical vapor deposition, sol-gel processing and controlled crystallization from a glassy matrix are some of the well known and successful processes for synthesizing nanomaterials. Amongst them, FAST is one of the most widely used methods to develop nano-structured ceramics or ceramic matrix composites (CMCs). Here it should be mentioned that one of the major disadvantages of conventional sintering techniques is the problem of grain growth encountered during sintering at high temperatures for longer holding times. It was widely found that fully dense materials had micron-sized grains, whereas retention of nano-sized grains resulted only in partial densification [12]. Hence, with the objective of achieving high densification while restricting grain growth, research efforts have been directed towards the development of novel sintering techniques. The advent of Spark Plasma Sintering (SPS), one of the variants of FAST, is one of the achievements from such efforts. Till date, many nanoscaled ceramics and CMCs have been successfully consolidated from nanosized starting powders via SPS route.

In this review, we discus the various classifications of ceramic nanocomposites in section 2. Section 3 deals with the challenges involved in the processing of bulk nanocrystalline ceramics followed by a brief mention of the sintering techniques that are successful in consolidating successfully bulk nanoceramics composites in section. The models related to improve-ment in mechanical properties of nanocomposites over conventional ceramics are discussed in section 4. Section 5 surveys the processing-microstructure-properties of nanocomposites developed via an advanced sintering technique (SPS) in some important ceramic systems like Al_2O_3 and Si_3N_4. Considering the fact that heavy duty wear encompasses an area of major application for structural ceramics, the tribological properties of nanoceramics and nanoceramic composites will be compared with the conventional materials in section 6. Finally, this review will conclude with raising some important issues, which remain unresolved in research on nanoceramics.

Classification of Nanocomposites

The term 'nanomaterials' encompasses a wide variety of revolutionary materials. Hence for convenience it is essential to subdivide them into various groups based either on their dimensions or microstructures. Based on dimensions [13], nanomaterials can be classified as: zero dimension (for example, clusters), one dimension (for example, single crystalline multilayers), two dimensions (for example, filamentary rods) and three dimensions (for example embedded nanoparticles or nano-composites). The present review will mostly be concentrated on nanocomposites, and in particular ceramic nanocomposites.

Ceramic nanocomposites were first developed in Japan, mainly by K. Niihara, claiming that ceramic materials with excellent mechanical properties can be obtained through nanocomposite technology [14]. Niihara classified ceramic nanocomposites into two broad categories: i) nanocomposites, fabricated by dispersion of nanosized particles within micron-sized matrix grains or at the grain boundaries of the matrix, and ii) nano/nanocomposites, in which matrix grains also are in the nanosized scale.

More extensively, the different nanoceramic composites can be classified as follows: (a) Intergranular nanocomposites, where the nanosized reinforcements are present at the grain boundaries and triple junctions of the matrix grains. The reinforcements pin the grain boundaries from migration and hence result in improved creep resistance. (b) Intragranular nanocomposites, which contain the nanoscaled reinforcements within the matrix grains, leading to high strength and toughness at room temperaure. (c) Inter/Intragranular nano-composites, where the nanosized reinforcements are present at the grain boundaries, triple junctions as well as within the matrix grains. These nanocomposites show a combination of properties of the first two classes. The hardness, toughness, strength, fracture resistance for creep and fatigue at high temperatures as well as the thermal shock fracture resistance are strongly improved for these composites [15]. (d) Nano/Nanocomposites, in which case both the matrix and the reinforcement particulates are in the nanosized range. Apart from the above mentioned improvement in properties, owing to the presence of an extremely large volume fraction of grain boundaries, nano/nanocomposites are expected to exhibit superplasticity due to enhanced grain boundary sliding. These composites also exhibit superior machinability. (e) Nano/microncomposite: another composite architecture could be the dispersion of

micronsized particulates in nanosized matrix, as observed by Basu et al in the ZrO_2-30 vol% ZrB_2 system consolidated via SPS [16]. A schematic representation of various model nanocomposite structures is shown in Fig. 1.

Processing of Nanoceramics Composites

Challenges Involved in Processing

Processing of bulk nanoceramics composites has always remained a major challenge for the materials community.

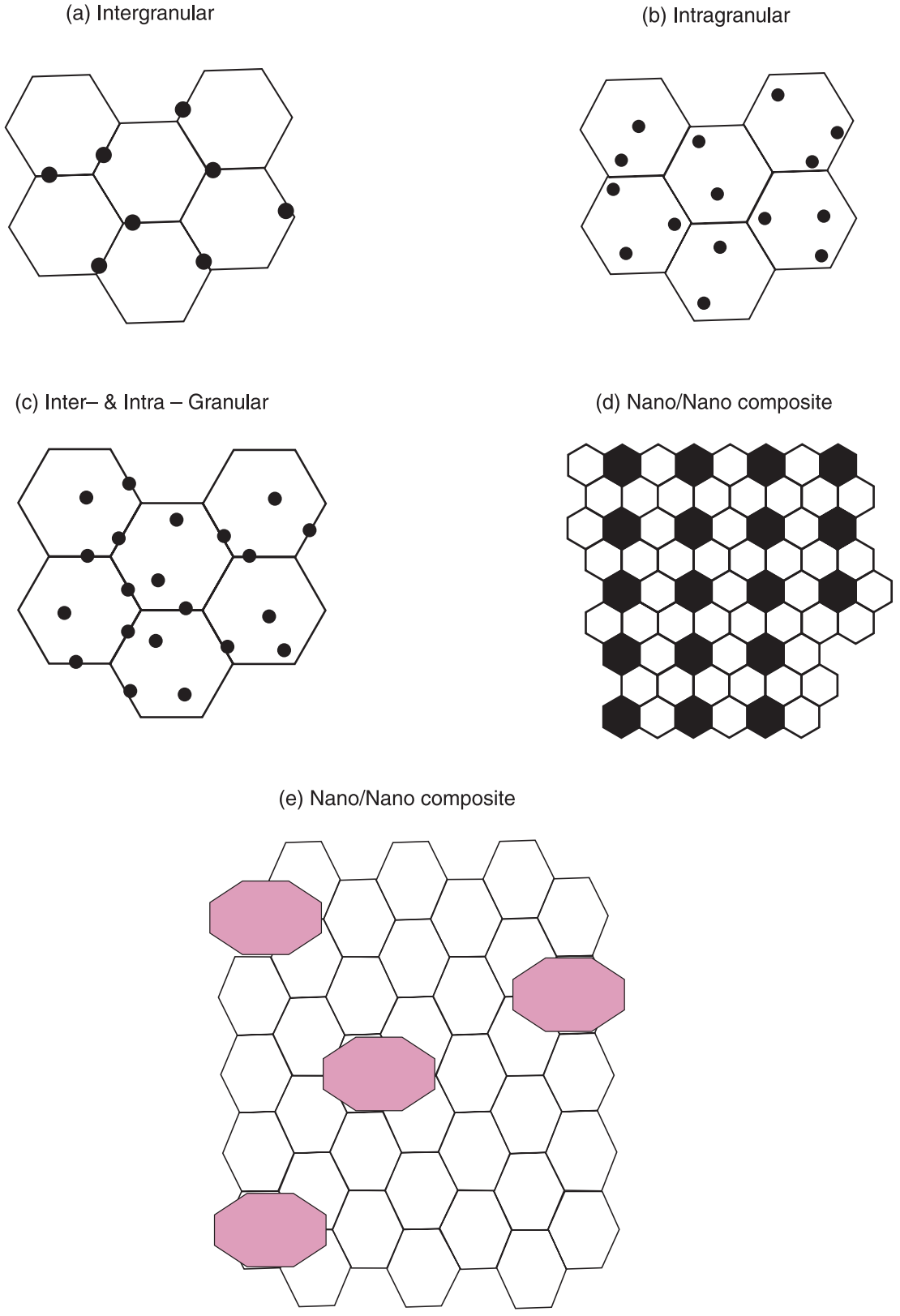

Fig. 1: *Schematic representation of the microstructural features of the various nanocomposites and nano-nano composites [14] and nano-micro composites [16].*

These challenges can be either due to the typical characteristics of the nanoscaled precursor powders or the limitations of the conventional sintering techniques to minimize grain growth during processing. Considering the problems associated with the powders; firstly, the synthesis of nanosized precursor powders require specialized techniques like inert gas condensation [15], sol-gel processing [17], high energy ball milling [18] and very careful process control. Secondly, a greater propensity of nano-sized powders to form strong agglomerates, due to the extremely high surface area to volume ratio, results in consolidation difficulties. Finally, their large interfacial areas make them susceptible to enhanced contamination by atmospheric adsorbates.

Problems of consolidating nanocomposites arise from the fact that the extremely high surface area to volume ratio of the nano-sized precursor powders result in a much higher driving force for grain growth, as compared to conventional coarser powders. The grain coarsening kinetics is given by:

$$G^2 - G_0^{\,2} = 2\alpha M_b \gamma_{gb} t \qquad (1)$$

where G is the grain size, G_0 the initial grain size, a is a constant, M_b is the grain boundary mobility, γ_{gb} the grain boundary energy and t is the time [19]. This equation shows that coarsening kinetics is enhanced with the increase in grain boundary/surface energy. In conventional sintering technique (pressureless sintering), a sintering temperature of around $0.7T_m$ is required to induce surface and volume diffusions. At such high sintering temperature and time, considerable grain growth occurs in the sintered nano-powders. Thus, it has been difficult to maintain nano-scaled grains in the final compact using conventional sintering techniques and it is understood that in order to materialize the promise of nanostructured materials, the problem of grain growth needs to be overcome.

Increased tendency for agglomeration of nanocrystalline ceramic powders also lead difficulties in minimizing grain growth during sintering. Smaller intercrystalline pores get annihilated much before the larger interagglomerate pores are removed. The absence of the intraagglomerate pores reduces the pinning action on grain boundaries and grain boundaries can move without much hindrance until they meet the widely spaced interagglomerate pores. Hence considerable grain growth occurs during further high temperature exposure required for removal of the interagglomerate pores.

Processes Used for Developing Bulk Ceramic Nanocomposites

The success in consolidation of nanopowders to yield bulk nanocomposites is strongly associated with the suppression of grain coarsening during densification. A combination of much lower sintering temperature and shorter sintering time, in short 'activated sintering', needs to be adopted in order to realize the dream of successfully synthesizing nanocomposites. 'Activated sintering' implies either increasing the driving force for sintering or making the process kinetically faster by physical or chemical treatment. This results in the increase of amount of densification with reduced sintering time and temperature.

The application of external pressure above the atmospheric pressure can result in increasing sintering kinetics and hence development of nanocomposites. This mechanism is utilized in conventional sintering techniques like hot pressing, sinter forging and hot isostatic pressing (HIPing). Increase of vacancy flux and plastic flow due to grain boundary sliding at high temperatures have been cited as the reasons for enhancement of densification kinetics of nanoceramics on application of pressure.

Another form of activated sintering, a novel process, which involves imposition of electric field simultaneously with applied pressure during densification is called Field Assisted Sintering Techniques (FAST) and is also known as Spark Plasma Sintering (SPS) or Plasma Activated Sintering (PAS) in Japan [20,21]. A schematic representation of the SPS set-up is shown in Fig. 2. The electric discharges, generated between the powder particles as well as the possible plasma formation, as a result of the applied electric field can potentially lead to an increase in the diffusion and densification kinetics. The cleaning of powder surfaces takes place due to thermal and electrical breakdown of the insulating surface films, which is caused either by due to high temperature, generated at the powder surfaces or the voltage exceeding the breakdown voltage of the films. The fast heating rates, those are achievable in SPS process, favor densification

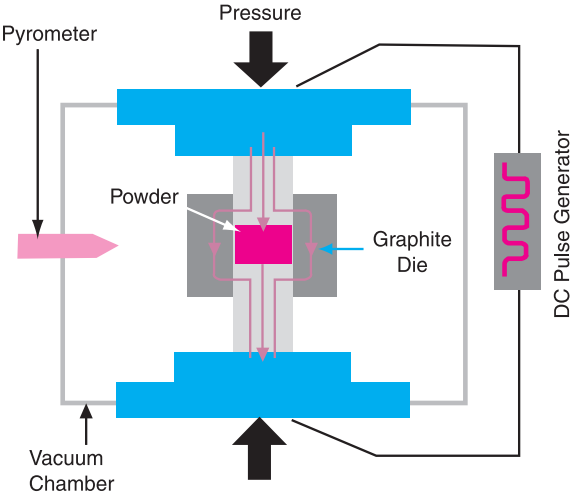

Fig. 2: *A schematic view of the SPS equipment*

over grain growth at the final stage of sintering. Chou et al. developed the following equation relating grain growth with heating rate:

$$G^m(T) = G_0^m + (g_o/\alpha)(\int_{To}^{T} \exp(-Q_g/KT)dT) \quad (2)$$

where G_0 is the starting grain size at time $t = t_0$, m is a constant, g_0 is a material constant, α is the constant heating rate, Q_g is the activation energy for grain growth, K is the Boltzmann constant, T is the absolute temperature [22]. This equation clearly shows that with higher heating rates (α), grain growth is suppressed. A high heating rate does not allow enough time for surface diffusion, to coarsen the structure at low temperatures and high temperatures are attained quickly. Due to this, in FAST, even coarsening sensitive materials (Al_2O_3, ZnO etc.), which have higher activation energy for diffusion than for grain growth, can be densified without significant grain coarsening [23]. Some examples of the grain sizes achieved in compacts consolidated via FAST synthesis from nanosized precursor powders are given in Table 1.

Table 1. Grain sizes obtained on FAST sintering of nanocrystalline monolith and composite powders.

System	Initial particle sizes (nm)	Final matrix grain sizes (nm)	Reference
γ-Al_2O_3/20 vol% 3Y-TZP	—	96	G. D. Zhan et al [44].
γ-Al_2O_3/20 vol% SiC_w	32	118	G. D. Zhan et al [41].
Mullite-10 vol% SiC	100	240	L. Gao et al [49].
Si_3N_4- 30 vol% TiN	5-20	50	Yoshimura et al [58].
ZrO_2-10 mol% Al_2O_3	<10	<100	M.Yoshimara et al [67].

Mechanical Properties of Nanoceramic Composites

Due to the success in developing nanoceramics and nanoceramic composites it has been possible to understand their mechanical behavior and derive the benefit of higher strength, hardness and modest increase in fracture toughness as a result of their ultra-fine grain sizes and nanoscaled reinforcements. It has been observed that though nanocrystalline materials are inherently stronger than their microcrystalline counterparts, yet the increment in strength falls below the estimated strength based on the Hall-Petch equation. The failure of Hall-Petch equation at the ultra-fine grain sizes is related to the fact that at these nanocrystalline grain sizes hardly experience any dislocation pile-ups, which form the basis of the theory of Hall-Petch equation. While the suppression of dislocation generation and motion with grain refinement is expected to cause nanocrystalline materials to be extremely strong, it is often found that at the finest grain sizes, a softening mechanism takes over as deformation by diffusional accommodation becomes significant. Thus further refinement after a critical grain size often results in an inverse Hall-Petch slope, that is decrease of hardness with grain refinement, as has been observed in case of TiAl [24] and TiO_2 [25]. Moreover, if we recall the kinetics of coble creep as described by the following expression:

$$e = (B\sigma\Omega\delta D_b)/(d^3KT) \quad (3)$$

where e is the diffusion creep rate, B is a constant, σ is the applied stress, Ω is the atomic volume, δ is the effective grain boundary thickness and D_b is the grain boundary diffusion coefficient. It can be mentioned here that a study, published in Nature [26], predicted the possibility of brittle materials, exhibiting signs of room temperature plasticity/deformability on grain refinement down to 100 nm. However, subsequent research [27], aimed at reconfirming room temperature deformability for nanocrystalline ceramics, have been mostly unsuccessful. Inspite of room temperature deformability being not yet demonstrated. Nevertheless, it has further been hypothesized that some brittle ceramics can behave superplastically at their application temperatures, if their grain sizes are reduced to nanoscale. In fact, such superplastic behavior has been observed in some nanocrystalline ceramic systems, such as polycrystalline tetragonal zirconia [4], TiAl [28], TiO_2 [29] and Si_3N_4/SiC [7]. Grain boundary sliding and augmented coble creep rate, arising from considerable increase in interfacial area, are the proposed mechanisms of the observed superplastic behaviour. However, it must be noted that, in spite of initial expectations, till date there has not been any extensive report on superplastic behavior of nanocrystalline ceramics at considerably lower temperatures, although nanocrystalline 5Y-TZP [30] and TiO_2 [29] has been observed to undergo extensive superplastic deformation at temperatures of around 1000^0C.

Nanoscaled reinforcements in ceramic nanocomposites have been found to result considerable increment in fracture resistance properties, in particular strength [31-34]. High temperature properties [33] as well as fracture toughness [34] are also enhanced to a modest extent in ceramic nanocomposites, in comparison to monolithic ceramics. Various examples, illustrating the improved properties of ceramic nanocomposites will be cited and discussed in following sections. Various models have been proposed to account for the improvement in properties [35]; which include, a) Matrix grain refinement due to grain boundary pinning by nanosized reinforcements and concomitant reduction in microstructural scale, b) Reduction in processing induced flaw sizes, c) Crack deflection due to compressive residual stresses, induced in the nano-reinforcements, owing to co-efficient of thermal expansion mismatch (change in fracture mode from intergranular to

Table 2. Mechanical properties of the various nanoceramics and nanocomposites processed via SPS and of the similar compositions processed via conventional sintering techniques

System (material)	Processing conditions	Heating rate (K/min)	Grain sizes (nm)	Hardness (GPa)	Toughness ($MPam^{1/2}$)	Strength (MPa)	Remarks	References
Monolithic alumina	High Pressure sintering	_	152	_	3.0	_	Nanocrystalline monolithic alumina showing lower toughness.	R.S. Mishra et al. [42]
γ-Al_2O_3/20 vol% 3Y-TZP	SPS at 1100^0C for 3 mins	500	α-Al_2O_3: 96 ZrO_2: 265	15.2	8.9	_	Incorporation of near nanocrystalline zirconia results in high toughness increment.	G.D. Zhan et al. [44]
γ-Al_2O_3/20 vol% SiC_w	SPS at 1125^0C for 3 mins	500	γ-Al_2O_3: 500	26.1	6.2	_	Nanocrystalline grains of alumina increases hardness while whisker reinforcement improves toughness.	G.D. Zhan et al. [41]
Al_2O_3-5 Vol% SiC	SPS at 1450^0C with no holding time	600	Nano-SiC	19	4	980	Intragranular nano SiC dispersions led to tremendous increase in strength.	L. Gao et al. [47]
SiC-ZrO_2 (3Y)-Al_2O_3	SPS at 1450^0C with no holding time	600	Nano-SiC	18	5	1200	Intragranular nano SiC dispersions led to tremendous increase in strength.	L. Gao et al. [48]
Al_2O_3 - 9 vol% $Nd_2Ti_2O_7$	SPS at 1100^0C for 3 mins	200	γ-Al_2O_3: 281 and nano-crystalline	_	5.67 ± 0.36	_	Toughening due to nano-scaled piezoelectric reinforcements.	G.D. Zhan et al. [45]
γ-Al2O3 - 7.5 vol% $BaTiO_3$	SPS at 1150^0C for 3 mins	200	α-Al_2O_3: 190 and nano-crystalline $BaTiO_3$	_	5.26 ± 0.34	_	Toughening due to nano-scaled ferroelectric reinforcements.	G.D. Zhan et al. [43]
Binderless WC	PAS at 1963 K for 0.18 Ks		25	23	4	_	Tremendous increase in hardness due to presence of nanocrystalline grains.	M. Sherif El-Eskandarany et al. [68]
WC-6 wt% ZrO_2	SPS at 1300^0C for 5 mins	600	WC: 300-400 ZrO_2: 100	23-24	6	_	Nanocrystalline microstructure and replacement of metallic binder with ceramic reinforcement increases hardness.	B. Basu et al. [62]
WC-18 wt% MgO	PAS at 1963 K for 0.18 Ks		MgO: 50 nm	15	14	_	Combination of high hardness (due to nanocrystalline microstucture) and toughness (due to MgO).	M. Sherif El-Eskandarany et al. [68]
ZrO_2-30 vol% ZrB_2	SPS at 1200^0C for 5 mins	600	ZrO_2: 100-300 ZrB_2:2000-3000	14	9.9	_	Presence of nano-sized matrix grains and hard reinforcements improve hardness.	T. Venkateswaran et al. [16]
SiC (5 vol%)-mullite	SPS at 1500^0C	200	Submicron mullite and nanocrystalline SiC	_	2.2-2.3	466	Presence of nano-SiC reinforcements led to strength increment from that of monolithic mullite (200-300 MPa).	L. Gao et al. [49]
YAG-5 vol% SiC	SPS at 1550^0C for 1 min	200	YAG: 1000 and nanocrystalline SiC	_	_	565	Nano-SiC reinforcements increased strength from that of monolithic YAG (348 MPa).	L. Gao et al. [50]
SiC-30 vol% TiC	SPS at 1800^0C for 20 mins	200 upto 600^0C, 150 from 600^0C to 1700^0C and 10 from 1700^0C to 1800^0C	Nanocrystalline TiC	_	6.2 ± 0.6	646.2 ± 11.3	Dispersions of nano-TiC lead to transgranular fracture SiC grains, resulting in improvement of bend strength, while intergranular fracture of TiC resulted in the improvement of fracture toughness.	Y. Luo et al. [51]

transgranular) and d) Strengthening of the grain boundaries due to the residual stresses generated on cooling from sintering temperature.

It is to be noted that although the effect of residual stresses due to the presence of second phase reinforcements are present in conventional ceramic microcomposites, yet the mechanical property improvement, resulting from such effects are much more pronounced in the case of ceramic nanocomposites. As analysed by Niihara [36], the reasons are three fold: Firstly, residual stresses, generated due to the presence of second phase reinforcements lead to a competition between toughening from particle bridging and toughness reduction due to residual traction in the matrix. Both these effects are a function of the average reinforcement dimension, which is represented graphically in Fig. 3a. Fig. 3a shows that although toughness increment due to particle bridging increases with increase in reinforcement size, it increases steeply upto particle size of ~ 100 nm and then flattens out considerable. On the other hand, the toughness reduction due to residual traction increases monotonically with increase in reinforcement size. As a result, the net toughness of nanocomposite initially increases with reinforcement size of upto ~ 100 nm and beyond such length scale, further increase in particle size lead to a reduction in the net toughness. Secondly, since it has been observed that crack propagation in most investigated ceramic nanocomposites (e.g Al_2O_3-SiC nanocomposite [36]) is via fracture of the matrix/reinforcement interface, an increase in interfacial strength is likely to result in impedance to crack propagation. Also, a reduction in reinforcement dimension to nanoscale leads to an increase in the interfacial strength due to good lattice matches observed in ceramic nanocomposites as opposed to that in the conventional microcomposites. A better lattice match, resulting from nanosize effect, is due to the fact that atomic diffusion through much smaller distance is capable of leading to near equilibrium structure. Thirdly, at a fixed reinforcement volume fraction, the interparticle distance (λ) decreases on reduction of particle sizes. Considering crack bridging as the major toughening mechanism, the frequency of interaction of crack with the second phase reinforcement increases considerably due to a reduction in λ. This has been the case, when second phase reinforcements are of nanosize. The tortuous nature of crack and frequent impedance to crack propagation leads to a steeper slope of R-curve (crack growth resistance curve) in the nanocomposites, as compared to that in microcomposites or monolithic ceramics (Fig. 3b).

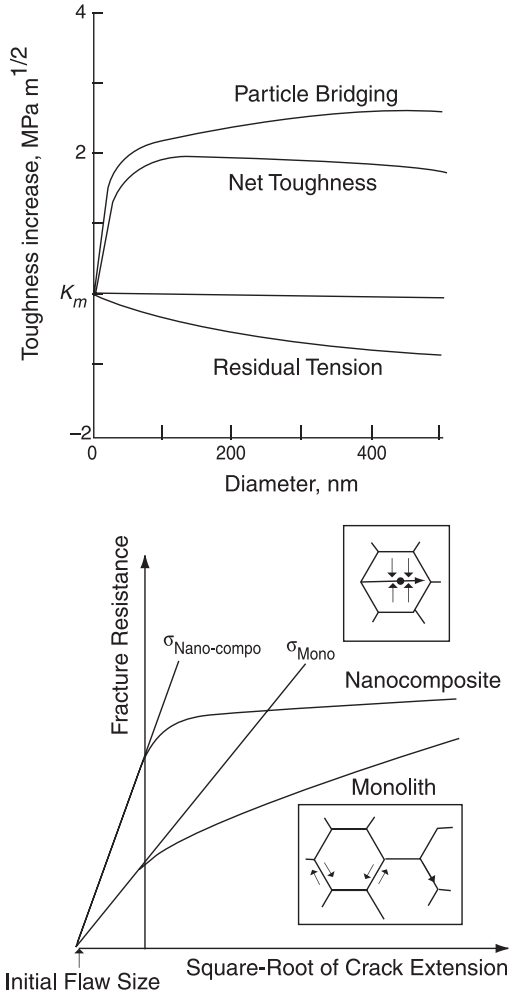

Fig. 3: *Plot depicting reinforcement diameter dependencies of the bridging-induced toughness increase, the residual-tension-induced toughness reduction, and the combined net toughness (a) and comparison of R-curve behavior of monolith and ceramic nanocomposite (b) [36].*

Nanoceramic Composites Processed via Advanced Sintering Techniques

When nanoceramic composites came to the fore, they were mostly developed using hot pressing as the primary consolidation technique [37,38]. Subsequently, the advent of SPS gave an impetus to the development of bulk nanocrystalline ceramics and ceramic matrix composites. Rapid heating to sintering temperature as well as lower sintering temperature and reduced holding time in SPS result in good control of the final grain size, such that nanoscaled microstructure is retained in the final compacts. In discussions that follow, we refer materials having grain sizes, of at least one of the phases, less than about 250 nm as nanocrystalline materials. Mechanical properties of the various nanoceramics and nanocomposites processed via SPS and of the similar compositions processed via conventional sintering techniques are presented in Table 2.

Nanocomposites Based on Alumina

It has been critically noted that in comparison to other oxide ceramics, densification of monolithic alumina to near theoretical density, while at the same time maintaining nano-scaled microstructure is really difficult

even using some of the advanced sintering techniques. One can observe in Fig. 4 that alumina requires comparatively higher homologous temperature for densification. Moreover, the densification behavior of alumina is strongly dependent on the crystal structure of the precursor powders [39]. Densification of γ-alumina is sluggish, possibly due to the nucleation controlled phase transformation from γ to α-alumina, which is detrimental to densification [40]. Thus, even higher homologous temperature is required to densify γ-alumina, as compared to other α-alumina and this results in significant grain growth.

With the advent of SPS, it has been possible to densify monolithic alumina to near theoretical densitiy, containing sub-micron as well as near nano-crystalline grains. Moreover, densification of γ-alumina precursor powders has been possible at a lower temperature than that of the γ to α transformation temperature (1200°C) [41]. However, attention must be given to the fact that such microstructural refinement does not lead to noticeable improvement of fracture toughness. For example, Mishra et al. found that alumina, with an

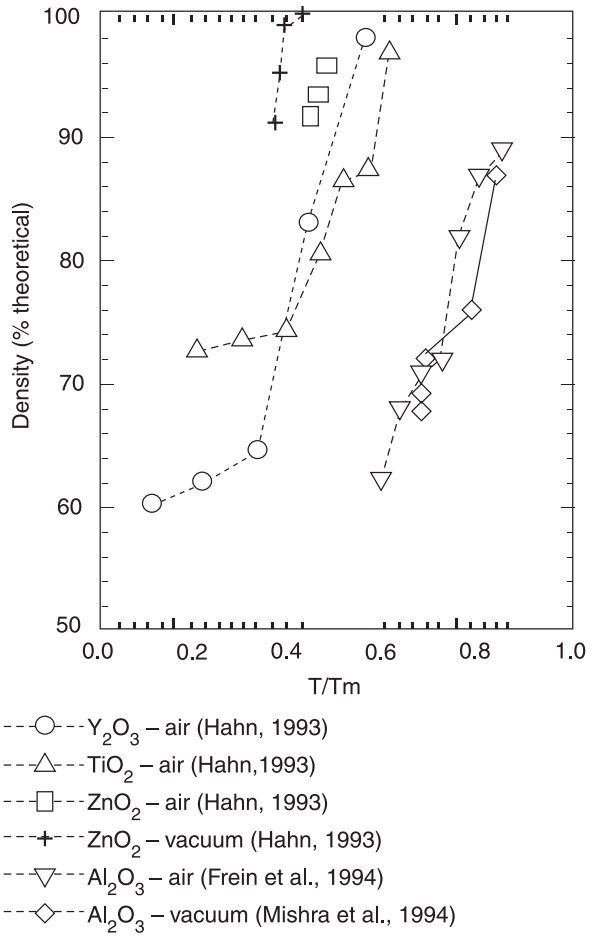

Fig. 4: *A comparison of the variation of density with homologous temperatures for various nanocrystalline metal oxides. Note that alumina requires the highest homologous temperatures for densification which makes it difficult to obtain high density nanocrystalline alumina [39]*

average equiaxed matrix grain size of 152 nm, exhibits a modest fracture toughness of around 3.03 MPam$^{1/2}$ [42]. It may be noted that similar observation regarding fracture toughness has been made for other ceramic systems. It needs a mention that toughness of ceramics correlates with the obstruction to crack propagation. Various crack shielding mechanisms are responsible for toughness enhancement in ceramic materials. Some conventional toughening methods, involving bridging zone mechanisms (particle bridging, ductile metal bridging, whisker/fibre pull out) as well as process zone mechanisms (transformation toughening of ZrO_2, ferroelastic domain switching in $BaTiO_3$ [43] and ZrO_2 [44], as well as piezoelectric toughening in $Nd_2Ti_2O_7$ [45] result in toughness enhancement of ceramics. However, simple reduction of grain size to nanoscale dimensions can contribute to enhanced frequency of crack deflection for intergranular fracture resulting in more crack path totuosity along with grain pull out, and such mechanisms can only enhance toughness to a very limited extent. Therefore, microstructural engineering is required in addition to grain refinement if increment in toughening is desired. Such microstructural modifications include reinforcement by second phase particles (composite formation) and as has been discussed previously (see section 4), nanocomposite approach results in much improvement in fracture resistance properties as compared to conventional composite formation.

In order to obtain alumina based ceramics with improved strength as well as higher toughness, similar nanocomposite approach has been proved to be highly beneficial. It is to be noted that Niihara et al. obtained modest toughness improvements upto ~ 4.7 MPa m$^{1/2}$ on reinforcing Al_2O_3 matrix with 5 vol% SiC nanoparticles [46]. In addition to enhancement of toughness extremely fine reinforcements within the matrix grains have been found to enhance the strength of alumina almost three times (1 GPa as compared to 350 MPa for monolithic Al_2O_3) due to residual stress strengthening of the grain boundaries [47]. At this point, it must be mentioned that the flexural strength of ceramics critically depends on the presence of surface flaws on the as-machined test sample. Therefore, a comparison in strength value would be appropriate, when all the tested samples were machined to standard bend samples. When the strength data are cited from the same reference [47], it is expected that the strength measurements were carried out on test samples with identical dimensions and similar surface finish.

We now look into a survey of some of the demonstrative reports pertaining to the sintering conditions, mechanical properties and underlying mechanisms involved in property improvements of Al_2O_3-based nanocomposites, synthesized via SPS.

(1) Zhan et al. [44] developed zirconia toughened alumina nanocomposite via combination of High Energy Ball Milling (HEBM) and SPS of the γ-alumina powders mixed with 3 mol% yttria stabilized zirconia (3Y-TZP). The obtained nanocomposite, SPSed at 1100^{0}C (heating rate of 500^{0}C/min), is characterised by a fine microstructure with alumina matrix grain size of 96 nm and the zirconia reinforcements having a size of 265 nm. SPS of pure alumina nanopowders at 1150^{0}C resulted in full densification with an average grain size of 349 nm in the compact. The hardness of approximately 15.2 GPa was measured for Al_2O_3-20 vol% ZrO_2 nanocomposite. The toughness values were around 8.9 MPam$^{1/2}$, which are three times higher than the toughness of monolithic alumina. It was concluded that the observed increment in toughness was due to ferroelastic domain switching of t-ZrO_2, and not stress induced tetragonal to monoclinic phase transformation (transformation toughening) in nanocrystalline zirconia.

(2) SPS at 1450^{0}C with a heating rate of 600^{0}C/min, with no holding time, at a pressure of 40 MPa, of heterogeneously precipitated 5 vol% SiC-Al_2O_3 powders resulted in fully compacted intragranular ceramic nanocomposite [47]. Nano-scaled SiC reinforcements were found to be uniformly distributed mostly within the Al_2O_3 grains. Figure 5a shows a TEM micrograph of the nanocomposite. The obtainment of finer microstructure and dispersion of nano-SiC enhanced the strength to as high as 980 MPa, which is much higher than 350 MPa normally observed in case of monolithic Al_2O_3. This finding was in agreement with the earlier finding of Niihara that incorporation of small amounts (5-10 vol%) of nano-scaled SiC reinforcements into alumina matrix drastically enhanced the strength to around 1000 MPa [14]. The toughness of the developed composite was around 4 MPam$^{1/2}$, which was slightly superior to that of monolithic alumina (3.5 MPam$^{1/2}$). A high hardness of around 19 GPa, similar to that of pure alumina, was also measured in the developed nanocomposite. The intragranular SiC particles resulted in tensile residual stress within the grains, thus weakening them for crack propagation, while corresponding compressive residual stress strengthened the grain boundaries, which resulted in fracture mode of the composite being transgranular in nature.

(3) SiC-ZrO_2(3Y)-Al_2O_3 nanocomposites were prepared from heterogeneously precipitated powders via SPS. Near theoretical density was achieved at 1450^{0}C (heating rate: 600^{0}C/min), without holding, using 40 MPa pressure. The optimised SPS temperature was about 200^{0}C lower than the optimised hot pressing temperature to obtain similar density. In the alumina matrix composite, the bend strength reached around 1.2 GPa, which is extremely high in comparison to that of pure alumina (350 MPa). The residual stress due to thermal expansion coefficient mismatch between Al_2O_3 and SiC was the key factor in achieving enhanced strength. The hardness of the composite was reported to be around 18 GPa. The nano-scaled SiC particles were located mainly within the matrix (Al_2O_3) grains, whereas ZrO_2 was distributed within as well as at the grain boundaries [48].

(4) In order to develop Al_2O_3 based nanocomposites with higher toughness, whisker reinforcement was utilized in developing 20 vol% SiC_w/γ-Al_2O_3 nanocomposites [41]. To overcome the densification difficulty of γ-Al_2O_3, finer starting powders (32 nm) along with mixed SiC whiskers (aspect ratio 5-100) were subjected to High Energy Ball Milling (HEBM). SPS sintering at 1125^{0}C (heating rate: 500^{0}C/min) for 3 mins at a pressure of 63 MPa resulted in the attainment of 99.8% densification. Thus using SPS the consolidation was done at a temperature lower than the γ to α-Al_2O_3 transformation temperature (1200^{0}C), which avoided the consolidation difficulties arising due to the transformation and enabled retention of γ-Al_2O_3 grains in the final microstructure. The matrix grains were around 118 nm in size. Whisker reinforcement approach and retention of nanoscaled final grain sizes resulted in a higher toughness of 6.2 MPam$^{1/2}$, while the reported hardness was also impressive (26.1 GPa).

Other Advanced Ceramic Nanocomposites

In addition to the above mentioned nanoceramics and nanocomposites, use of SPS and related techniques has made it possible to develop a variety of technically important ceramic materials having nano-scaled microstructures. Also SPS can be used for other purposes apart from simple consolidation. A few examples are cited below, which gives a further glimpse of the wide field of application of FAST sintering techniques.

Mullite/SiC: Gao et al. [49] attained nearly full densification on SPS processing of SiC (5 and 10 vol%)-mullite nanocomposites. The temperature required was 1500^{0}C, which was much lower than that required in conventional sintering of mullite (1600^{0}C-1700^{0}C). The nano-SiC particles were found to be located within the matrix grain (intragranular ceramic nano-composite. Considerable dislocation activity was found in the vicinity of the SiC particles due to thermal stresses generated during cooling. A notable feature was the atomically clean grain boundaries obtained between the mullite grains as well as between the SiC and mullite grains, thus confirming the surface cleaning effects of the electric discharges generated in FAST densifications.

The measured flexural strengths (466 MPa and 454 MPa for 5 vol% and 10 vol% SiC reinforcements respectively) were much higher than that (200-300 MPa) of the mullite monoliths. The residual stresses generated and the generation of dislocations were accounted for the increment of strength. However, the fracture toughness (2.2-2.3 MPa $m^{1/2}$) did not improve in the nanocomposites as compared to mullite monoliths (2-2.5MPa $m^{1/2}$).

YAG/SiC: Incorporation of nano-sized SiC particles into Yttrium aluminium garnet (YAG), has been reported to considerably improve its mechanical properties. YAG - 5 vol% SiC nanocomposites, fully densified by SPS (at 1550^0C) exhibited high bend strength of 565 MPa, which is higher than that of pure YAG (348 MPa), consolidated using SPS. Incidentally both the values are higher than the reported bend strength (238 MPa) of hot pressed pure YAG. The nano-sized SiC dispersions were in the intragranular regions. Also, the and the fracture mode was transgranular, primarily due to residual stress strengthening of the grain boundaries [50].

SiC/TiC: The SiC-based nanocomposites containing dispersions of nanosized 30 vol% TiC was sintered to near theoretical density using SPS at 1800^0C [51]. The composites had a fracture toughness of 6.2 ± 0.6 MPa $m^{1/2}$ and bend strength of 646.2 ± 11.3 MPa $m^{1/2}$. Investigation of the fracture mode revealed that transgranular fracture occurred in the SiC grains, which resulted in improvement of bend strength, while intergranular fracture of TiC resulted in the improvement of fracture toughness, since weak grain/interface boundaries enhance crack bridging intensities [52].

Si_3N_4/SiC Nanocomposites: Park et al. reported the development of Si_3N_4/SiC nanocomposites by hot pressing a mixture of Si_3N_4 and β-SiC at 1800^0C for 2 hours. In their experiments, heat treatment of powder mixtures at an optimized temperature (1400-1500^0C), prior to the densification was adopted [53]. It was reported that heat treatment at 1500^0C resulted in the development of a microstructure, characterized by the presence of a significant fraction of nanocrystalline SiC particles at the grain boundaries of the fine grained Si_3N_4 matrix. The developed nanocomposite with 20 vol% SiC nanocrystalline reinforcements exhibited high flexural strength (~ 1150 MPa) at room temperature, which was maintained upto 1200^0C. Hot pressed Si_3N_4/SiC nanocomposites, as developed by Oh et al. [54], are characterized by inter/intragranular nanocrystalline SiC. Such nanocomposites also exhibited similarly high strength of 1100 MPa at room temperature and maintained strength of 800 MPa at a high temperature of 1400^0C. In another work, dealing with the mechanical behavior of hot pressed monolithic Si_3N_4 and Si_3N_4/SiC nanocomposites, it was observed that the nanocomposites exhibit much improved strength and fracture toughness, at room temperature as well as elevated temperature [55]. These experimental results confirm that the limitations imposed on the high temperature strength by the amorphous grain boundary phase, can be alleviated by reducing the additive content while densifying them via SPS [56]. The densification of the amorphous Si-C-N with a reduced additive content (~ 1 wt% yttria) at a nominal temperature of 1600^0C, via predominantly solid state sintering, restricted grain growth of both the phases (Si_3N_4 and SiC) and hence led to the development of nano/nano ceramic composite.

Si_3N_4/TiN: Combination of mechanical milling of the powders and SPS resulted in the development of Si_3N_4/TiN nanocomposites [57]. Consolidated at 1673 K, 99% densification was obtained with the final microstructures having grains of dimensions around 50 nm. The starting powders had sizes between 5-20 nm and were milled for 16 hours. This once again proves the ability of SPS to suppress grain growth while achieving densification.

Tribological Properties of Nanocomposites

Due to the superior hardness, strength and chemical inertness of ceramics in comparison to other material classes, the structural ceramics are known to exhibit better wear and abrasion resistance. Further improvement of the wear behavior of ceramics can be possible by hardness increment due to reduction in grain sizes to nano scales. Nanoceramic composites are known to exhibit better strength and hardness than their microcrystalline counterparts. Moreover higher hardness should lead to reduced wear depth and higher resistance against abrasion. Ultra fine grain sizes often result in milder wear when grain pull out is the dominating mechanism due to reduced size of the debris formed. Higher strength and hardness result in slowing down of the plasticity induced damage accumulation. Moreover, reduction in flaw sizes in nanocomposites result in considerable increment in the critical stress required for brittle fracture controlled wear. Wear transition from mild to severe wear is also generally delayed in nanocomposites [58]. In nanocomposites, change in fracture mode from intergranular to transgranular also result in significant reduction in pull out rate and hence improvement of wear resistance. Inspite of such expectations, literature reports dealing with the tribological behavior of nanocomposites are limited. Comparison of tribological behaviour of various nanoceramics and nanocomposites is presented in Table 3.

Rodriguez et al. [59] reported two orders of magnitude higher wear resistance for Al_2O_3-(2-5 vol%) SiC nanocomposites as compared to unreinforced alumina. Nano-sized dispersions of SiC (40-800 nm) was

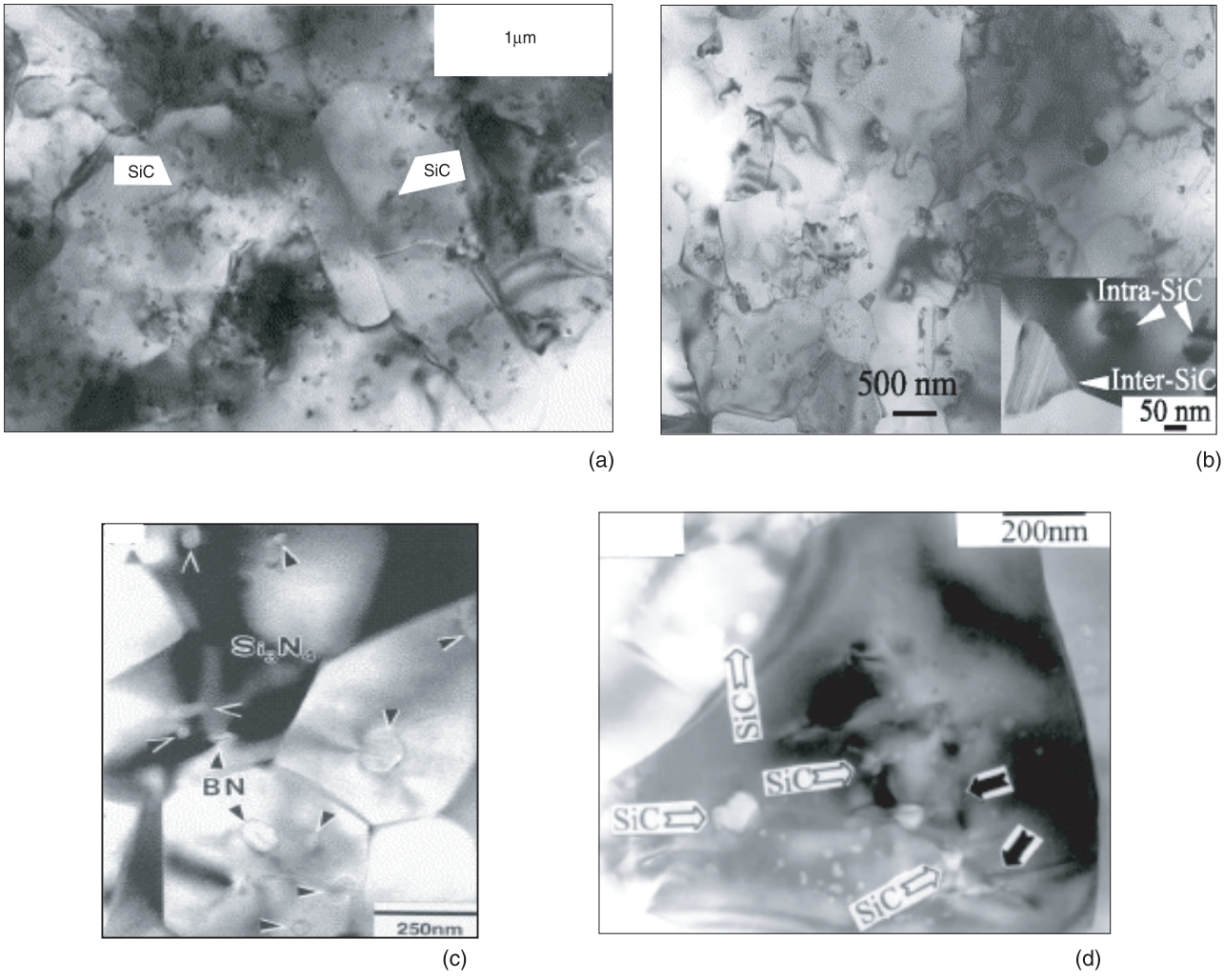

Fig. 5: *(a) TEM micrographs of ceramic nano-composites, showing microstructure of Al_2O_3-5 vol% SiC nanocomposites consolidated via SPS [47]; (b) Alumina-Silicon Carbide Nanocomposites consolidated via Reactive Hot Pressing [69]; (c) hot-pressed Si_3N_4/BN vol% nanocomposite processed through the chemical route [70]; (d) Mullite-5vol% SiC [49]*

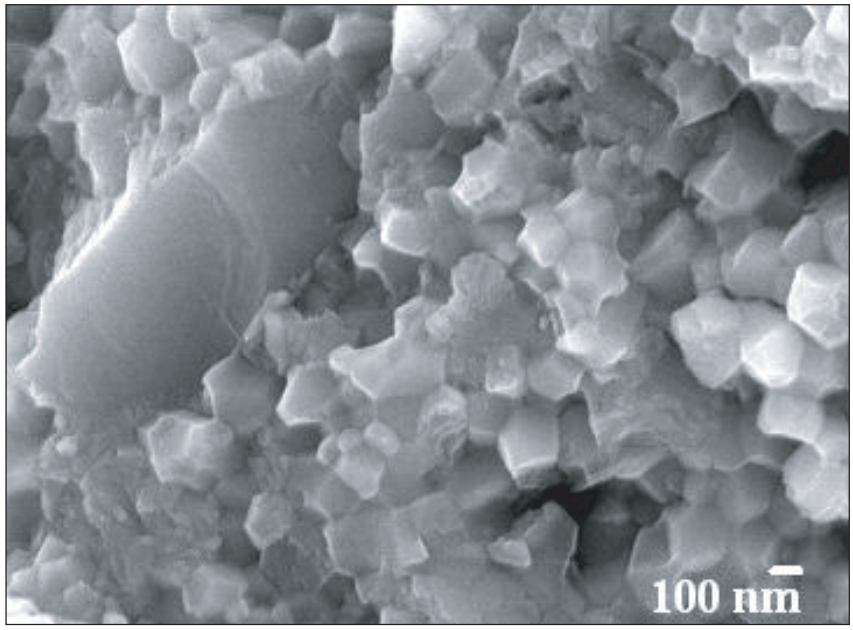

Fig. 5(e): *SEM fractograph of Spark plasma sintered ZrO_2-ZrB_2 nanoceramic composites, sintered at 1200°C for a holding period of 5 min in vacuum revealing a model ceramic nanocomposite microstructure with nanosized matrix particles reinforced with micron sized reinforcement particulates [16].*

reported to cause much improved tribological behavior against Mg-PSZ under sliding wear conditions at high normal loads (125-150 N). Similarly, Davidge et al. [60] observed significant reduction in erosive wear rate, accompanied by smooth transgranular fracture as a result of the dispersion of secondary nanoparticles of SiC in Al_2O_3 matrix. In a recent work comparing the wear behavior of alumina and Al_2O_3/SiC nanocomposites under abrasive wear conditions, it was shown that wear rate and area fraction of surface pull out were reduced considerably on increasing the amount of SiC dispersions and reducing the grain size of alumina [61]. It was concluded that at the highest SiC (10 vol %) content surface pull out was significantly reduced (Fig. 6). This is due to change in fracture mode from intercrystalline to transcrystalline on reinforcing with nanoscaled SiC particles and blocking of dislocations pile-ups and twins which otherwise provided stress necessary for the brittle fracture.

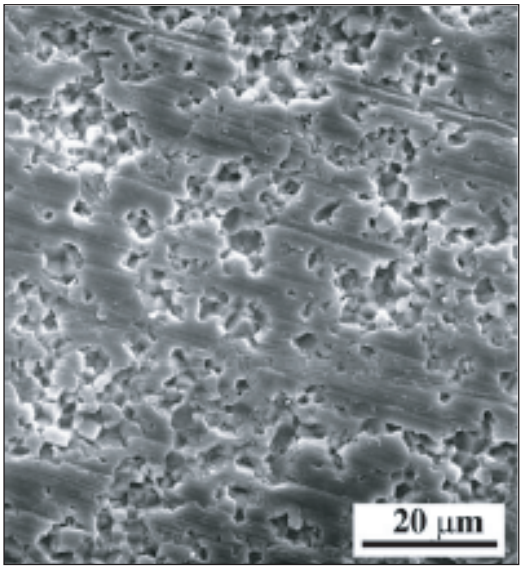

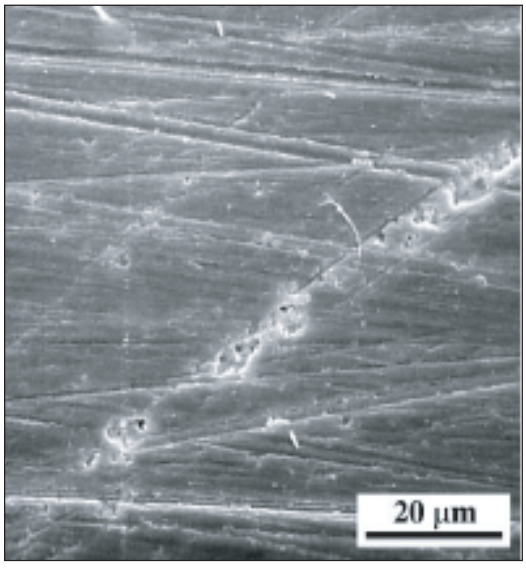

Fig. 6: *Selections of worn surfaces of monolithic Al_2O_3 and Al_2O_3/SiC nanocomposite showing pullout by brittle fracture and load bearing area with scratches indicative of plasticity-controlled wear; fine grained alumina showing predominantly intergranular fracture within the pullouts and (b) 10% SiC nanocomposite showing low density of small pullouts, associated with a minority of the scratches [61].*

Basu et al. [62] investigated the wear behavior of nanocrystalline 3Y-TZP compacted using SPS against commercial bearing grade steel ball (SAE 52100), under fretting condition. The study clearly revealed the influence of hardness/strength increment due to grain refinement on improvement of wear behavior. The sample sintered at 1200^0C via SPS exhibited minimum wear and the wear rate increased with increasing sintering temperature. Wear resistance was lowest for the sample conventionally sintered at 1450^0C (Fig. 7). Abrasive wear accompanied by microcracking, intergranular fracture and grain pullout (tribomechanical wear) was found to be the major mechanism for material removal in zirconia nanoceramics (Fig. 8a).

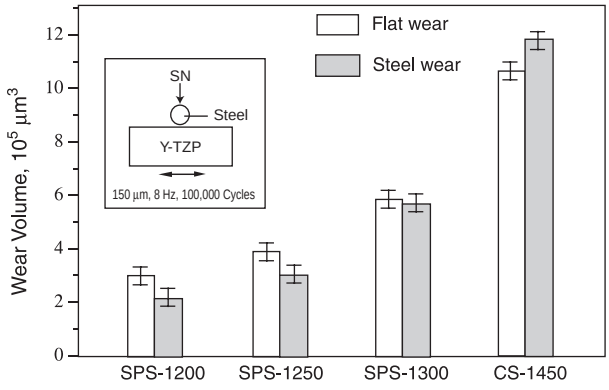

Fig. 7: *Wear volume as measured under unlubricated sliding conditions on a commercial fretting wear tester. The testing conditions and the counterbody (6-mm diameter steel ball) are shown in the inset. The comparison is made between the SPS-processed nanozirconia and the conventionally sintered (CS) zirconia. The error bars represent the standard deviation of at least three fretting tests [62]*

WC based composites are expected to show superior wear behavior since the major application of WC encompasses around wear resistance. Moreover if metallic binder of WC based cermets is replaced by ceramic additives, the resultant composites exhibit higher hardness and strength [63]. Basu et al. [64] investigated the wear behavior of the newly developed WC-6 wt% ZrO_2 nanocomposite consolidated via SPS. The wear behavior was studied under mode 1 fretting condition against a steel ball. It was found that the developed nanocomposite exhibited lower wear rate (~10^{-8} mm^3/N.m) as compared to the one pressureless sintered at 1600^0C (~10^{-6} mm^3/N.m) containing larger zirconia reinforcements. This was due to higher hardness of the SPSed composite having finer ZrO_2 grains. At lower loads (2N) a very low COF, that is 0.1, was observed,

though higher loads led to wear transition giving rise to higher COF (0.5) after long periods (50,000 cycles) of fretting. Tribochemical wear was the major mechanism of material removal at higher loads (Fig.8b).

Concluding Remarks

The present review has demonstrated the progress that has been made to develop several ceramic nanocomposites. In particular, considerable research efforts were invested in understanding the processing-microstructure-mechanical-tribological properties of nanoceramics and nanoceramic composites during the last few decades. Among advanced sintering techniques, SPS has emerged as a sintering technique capable of consolidating bulk nanocrystalline materials, by providing a high heating rate, lower sintering temperatures and short holding times benefited by applications of the pulsed electric current. Very little grain growth has been observed during densification to near theoretical density for a number of nano precursor powders. Though the inherent mechanisms of SPS are still under research, the promise of nanostructured materials seems to be fulfilled with the advent of SPS.

It can be concluded that experimental studies on the mechanical behavior of nanoceramics and nanoceramic compositions till date has proved that significant improvement of strength and hardness can result from the refinement of matrix grain sizes or incorporation of secondary nanosized reinforcements. This, in turn has led to an augmentation of the wear resistance of the ceramic materials, thus leading to increased tribological applications, which has necessitated the discussion on the recent reports on tribological properties of selected ceramic nanomaterials.

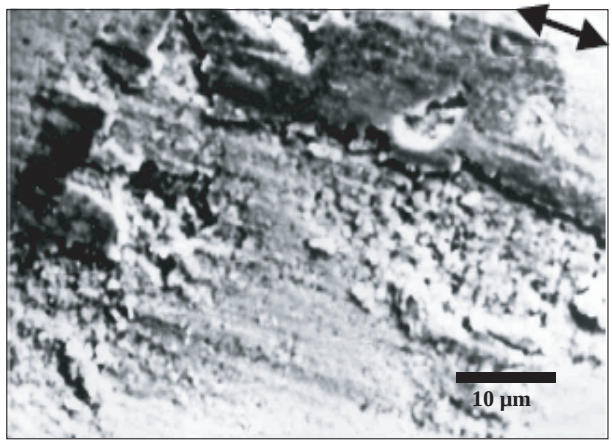

(a)

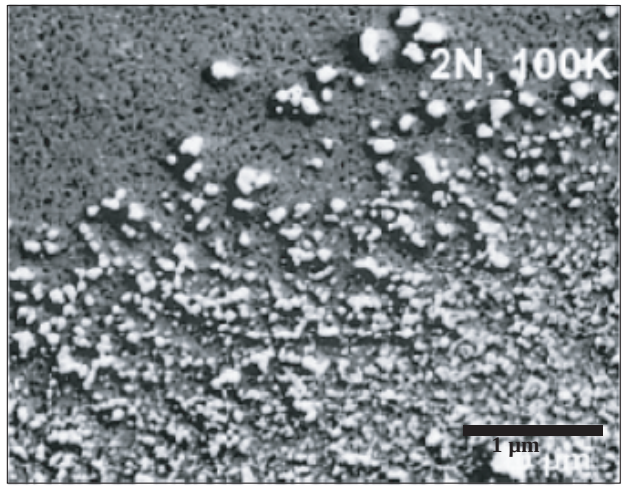

(b)

Fig. 8: *(a) SEM micrograph showing the evidence of intergranular cracking and grain pull out occurring at the worn surface on the nano-zirconia (SPS-1200 ceramic) after the fretting test at a load of 8 N, frequency of 8 Hz, duration of 100 000 cycles. The double pointed arrow indicates the sliding direction; (b) SEM image showing the generation of submicron sized wear debris during wear of WC-6 wt% ZrO_2 [64]*

Table 3. Comparison of tribological behaviour of various nanoceramics and nanocomposites

Material	Counterbody	Tribological conditions	COF	Wear rate (X 10^{-6}) (mm^3/N.m)	Wear Mechanisms	Reference
3Y-TZP	Bearing grade steel (SAE 52100)	Mode I Fretting wear with a normal load of 8 N, frequency 8 Hz, displacement stroke 150µm, duration 100000 cycles	0.5	1.25	Microcracking, intergranular fracture, grain pull out	Basu et al. [62]
WC- 6 wt% ZrO_2	Bearing grade steel (SAE 52100)	Mode I Fretting wear with a normal load of 2 N, frequency 8 Hz, displacement stroke 50µm, duration 100000 cycles	0.1	0.01	Mild oxidative wear, grain pull out	Basu et al. [64]
Al_2O_3-10 vol% SiC	Resin-bonded alumina plate with an oil-based suspension of 45 µm diamond abrasive	Abrasive wear test with rotation of the grinding plate at 350 rpm, under a constant load of 22.2 N	_	0.3 µm/s (the volume of material removed per unit contact area per unit time)	Material removal by plastic deformation and grain pull out	J.L. Ortiz-Merino et al. [61]

Inspite of such extensive research on ceramic nanocomposites till date, the factors leading to the improvements in mechanical properties are still not clearly understood. Only some theoretical models based on certain assumptions have been established. Even though considerable increment in strength and hardness has been obtained, room temperature fracture toughness in ceramic nanocomposites is still not satisfactory. The modest fracture toughness is an important factor in determining the tribological properties of brittle materials. Therefore, any substantial improvement in wear resistance requires similar improvement in fracture resistance properties. Hence, extensive research in the field of nanoceramics is required to develop new strategies to increase the fracture toughness. Hybrid composite development with optimized composition and microstructure seems to be one of the solutions.

Although nanoceramic composites have been developed in many technologically important ceramic systems, further studies should focus on understanding the mechanical–tribological property evaluation in order to confirm any specific advantage in wear resistance property due to nanoscale ceramic microstructure. Also, efforts should be invested to study the machinability and joining characteristics of structural ceramic nanocomposites.

Nevertheless, at higher temperatures, nanocrystalline ceramics are reported to exhibit superplasticity due to Coble creep as a result of increased interfacial area. In fact, Superplastic behavior of 3Y-TZP has been exploited in near net-shaping applications by forming ceramic tubes (Fig. 9) [65]. Even superplastic deformation of nanocrystalline Y-TZP at temperatures as low as 1150^0C has been exploited successfully in joining two zirconia ceramics [66].

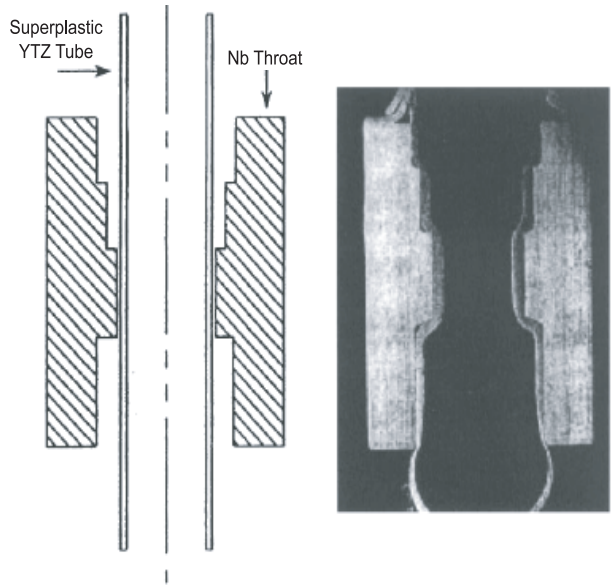

Fig. 9: *Schematic diagram of an experiment to expand superplastic YTZ tube within a rigid Nb shell (left); the cross-section after forming at 1550^0C (right) [66]*

References

1. V Ponec *Catal. Rev. Sci. Eng.* **11** (1975) 41
2. C R Martens (Eds) *Technology of Paints, Varnishes and Lacquers* (New York: Reinhold) (1968) 335
3. K S Kumar, H V Swygenhoven and S. Suresh *Acta Materialia* **51** (2003) 5743
4. TG Nieh and J Wadsworth *Acta Metall Mater* **38** (1990) 1121
5. I Amato *Mater Sci Forum* **455-456** (2004) 550
6. GB Prabhu and DL Bourell *Scripta Met et Mat* **33[5]** (1995) 761
7. F Wakai and H Kato *Adv Ceram Matter* **3** (1998) 71
8. JMC Moreno, M Schehl and M Popa *Acta Materialia* **50** (2002) 3973
9. F Wakai, Y Kodama, S Sakaguchi, N Murayama, K Izaki and K Niihara *Nature* **344** (1990) 421
10. JP Borel *Surf Sci* **106** (1981) 1
11. MN Rahaman *Ceramic Processing and Sintering* 383
12. H Hahn, J Logas and RS Averback *J Mater Res* **5** (1990) 609
13. H Gleiter *Acta Materialia* (Millenium-Issue) **48** (2000) 1
14. K Niihara *J Ceram Soc Jap* The Centennial Memorial Issue **99[10]** (1991) 974
15. K Niihara and Y Suzuki *Mat Sc and Engg* **A 261** (1999) 6
16. B Basu, T Venkateswaran and DY Kim *J Am Ceram Soc* (accepted, in press 2006)
17. SH Yoo, TS Sundarshan, K Sethuram, G Subhash and RJ Dowding *Nanostruct Mat* **12** (1999) 23
18. GS Choi, JY Kim and DH Lee *J Korean Inst Met Mater* **30** (1992) 840
19. TR Mallow, CC Koch *Acta Materialia* **45** (1997) 2177
20. S Shiga, K Masuyama, M Umemoto and K Yamazaki in: RM German, GL Messing, RG Cornwall (Eds) *Sintering Technology* Marcel Dekker New York (1996) 431
21. Jones, JR Groza, K Yamazaki and K Shoda *Mater Manuf Proc* **9** (1995) 1105
22. MY Chu, MN Rahaman and LC DeJonghe *J Am Ceram Soc* **74** (1991) 1217
23. M Harmer, WW Roberts and RJ Brook *Trans J Br Ceram Soc* **78** (1979) 22
24. H Chang, CJ Alstetter and RS Averback *J Am Ceram Soc* **74** (1991) 2672
25. M Guermazi, HJ Hofler, R Hahn and RS Averback *J Am Ceram Soc* **74** (1991) 2672
26. J Karch, R Birringer and H Gleiter *Nature* **330** (1987) 556
27. WD Kingery, HK Bowena and DR Uhlmann *Introduction to Ceramics* **second edition** Wiley, New York (1976) 231
28. K Ameyama, A Miyazaki and M Tokizane *Superplasticity in advanced materials* S Hori (Eds), M Tokizane and N Furushiro (Japanese Society of Research on Superplasticity) (1991) 317
29. H Hahn and RS Averback *J Am Ceram Soc* **74** (1991) 2918
30. U Betz, G Scipione, E Bonetti and H Hahn *Nanostructured Materials* **8[7]** (1997) 845
31. C E Borsa, S Jiao, R I Todd and R J Brook *J Microscopy* **177** (1994) 305
32. RW Davidge, RJ Brook, F Cambier, M Poorteman, A Leriche, D O'Sullivan, S Hampshire and T Kennedy *J Eur Ceram Soc* **16** (1996) 799
33. T Hirano and K Niihara *Mater Lett* **22** (1995) 249
34. A Sawagushi, K Toda and K Niihara *J Am Ceram Soc* **74** (1991) 1142

35. M Sternitzke *J Eur Ceram Soc* **17** (1997) 1061
36. T Ohji, YK Jeong, YH Choa and K Niihara *J Am Ceram Soc* **81[6]** (1998) 1453
37. K Niihara, A Nakahira and M Inoue *Mater Res Soc Symp Proc* **271** (1992) 589
38. G Sasaki, T Suga, K Suganuma, T Fujita and K Niihara *Trans Mater Res Soc Jpn* **16B** (1994) 1517
39. R S Mishra and A K Mukherjee *Mat Sc and Engg* A287 (2000) 178
40. F W Dynys, J W Halloran *J Am Ceram Soc* **65** (1982) 442
41. GD Zhan, JD Kuntz, RG Duan and AK Mukherjee *J Am Ceram Soc* **87[12]** (2004) 2297
42. RS Mishra, CE Leshier and AK Mukherjee *J Am Ceram Soc* **79[11]** (1996) 2989
43. GD Zhan, J Kuntz, J Wan, J Garay and AK Mukherjee *Mat Sci and Engg* **A356** (2003) 443
44. GD Zhan, J Kuntz, J Wan, J Garay and A K Mukherjee *J Am Ceram Soc* **86 [1]** (2003) 200
45. GD Zhan, J Kuntz, J Wan, J Garay and AK Mukherjee *Scripta Materialia* **47** (2002) 737
46. K Niihara and A Nakahira *Ann Chim Fr* **16** (1991) 479
47. L Gao, HZ Wang, JS Hong, H Miyamoto, K Miyamoto, Y Nishikawa and S D D L Torre *J Eur Ceram Soc* **19** (1999) 609
48. L Gao, HZ Wang, JS Hong, H Miyamoto, K Miyamoto, Y Nishikawa, SDDL Torre *NanoStructured materials* **11[1]** (1999) 43
49. L Gao, X Jin, H Kawaoka, T Sekino and K Niihara *Mat Sc and Engg* **A334** (2002) 262
50. L Gao, H Wang, H Kawaoka, T Sekino and K Niihara *J Eur Ceram Soc* **22** (2002) 785
51. Y Luo, S Li, W Pan and L Li *Mat Letters* **58** (2003) 150-153
52. A Liana *J Am Soc* **82** (1999) 78
53. H Park, HE Kim and K Niihara *J Eur Ceram Soc* **18** (1998) 907
54. YS Oh, CS Kim, DS Lim and DS Cheong *Scripta mater* **44** (2001) 2079
55. YH Koh, HW Kim and HE Kim *Scripta mater* **44** (2001) 2069
56. J Wan, RG Duan and AK Mukherjee *Scripta Materialia* **53** (2005) 663
57. M Yoshimura, O Komura and A Yamakawa *Scr Mater* **44** (2001) 1517
58. HJ Chen, WN Rainforth, WE Lee *Scr Mater* **42** (2000) 555
59. J Rodriguez, A Martin, JY Pastor, J Llorca, JF Bartolome and JS Moya *J Am Ceram Soc* **82 [8]** (1999) 2252
60. RW Davidge, PC Twigg and FL Riley *J Eur Ceram Soc* **16** (1996) 700
61. LO Merino and RI Todd *Acta Materialia* (2005) article in press
62. B Basu, J H Lee and D Y Kim J *Am Ceram Soc* **87[9]** (2004) 1771
63. T S Srivatsan, R Woods, M Petaroli and T S Sudarshan *Powder Technology* **122** (2002) 54
64. T Venkateswaran, D Sarkar and B Basu *J Am Ceram Soc* **88 [3]** (2005) 691
65. J Wittenauer in: V A Ravi, T S Srivatsan, J J Moore (Ed.), "Processing and fabrication of advanced materials III"; *The Minerals, Metals and Materials Society* (1994) 197
66. FG Mora, AD Rodriguez, JL Routbort, R Chaim, F Guiberteau *Scripta Materialia* **41[5]** (1999) 455
67. M Yoshimura, M Sando, Y H Choa, T Sekino and K Niihara *Key Engg Mat* **423** (1999) 161
68. MSE Eskandarany *J Alloys and Compounds* **296** (2000) 175
69. Zhang, Yang, Ando and T Ohji *J Am Cer Soc* **87** (2004) 299
70. T Kusunose, T Sekino, Y H Choa and K Niihara *J Am Ceram Soc* **85 [11]** (2002) 2689